Technical Report: **Rayleigh Scattering Combustion Diagnostic**

Wyatt Adams
Dr. Ethan Hecht
Combustion Research Facility, Sandia National Laboratories, Livermore, CA
July 29th, 2015

Abstract

A laser Rayleigh scattering (LRS) temperature diagnostic was developed over 8 weeks with the goal of studying oxy-combustion of pulverized coal char in high temperature reaction environments with high concentrations of carbon dioxide. Algorithms were developed to analyze data collected from the optical diagnostic system and convert the information to temperature measurements. When completed, the diagnostic will allow for the kinetic gasification rates of the oxy-combustion reaction to be obtained, which was previously not possible since the high concentrations of high temperature CO_2 consumed thermocouples that were used to measure flame temperatures inside the flow reactor where the combustion and gasification reactions occur. These kinetic rates are important for studying oxy-combustion processes suitable for application as sustainable energy solutions.

Introduction

While it has been known for many years that increased atmospheric carbon levels due to human activity can produce a greenhouse effect in the Earth's atmosphere[1], fossil fuels such as coal and petroleum, due to their contribution to global warming, have only relatively recently attracted the negative attention necessary to produce new legislation and a meaningful shift in the way energy is produced[2]. Research on renewable energy solutions such as wind and solar has continued to accelerate, but fossil fuels still dominate the energy market due to their low levelized cost of energy compared to renewable sources[3]. Also, the need for new infrastructure to implement renewables and other sustainable energy solutions, especially for potentially viable transportation technologies such as hydrogen fuel cells, provides motivation for improving upon the existing methods of energy production until new technologies can be more economically competitive. For example, retrofitting coal-fired power plants to operate via oxy-combustion with flue gas recirculation combined with carbon capture and sequestration (CCS) could be a way to utilize fossil fuels without contributing to an increase in atmospheric carbon. While promising for the near future, new methods of utilizing fossil fuels (including oxy-combustion of coal, which is of specific interest to this report), present some of their own engineering challenges[4,5], and further research is required before such technologies are ready for widespread deployment.

Oxy-combustion, or oxy-fuel combustion, refers to the process of burning a fuel in the presence of high oxygen (O_2) concentrations instead of air, which is mostly composed of nitrogen (N_2). Since there is no significant volume of N_2 present in oxy-combustion to be wastefully heated, fuel consumption is reduced, higher flame temperatures are enabled, and the resulting flue gas has a high enough CO_2 concentration to be suitable for subsequent use and sequestration[6]. Previously, the CO_2 gasification reaction in the oxy-combustion of pulverized coal char has been studied to further explore the proposal that the CO_2 gasification reaction enhances the char burning rates in oxy-fuel combustion[7].. The desire to characterize this process presents a need to experimentally determine the kinetic gasification rate at temperatures relevant to oxy-combustion, which requires information about the reacting gas temperature. An ongoing experiment at the Combustion Research Facility (CRF) at Sandia National Laboratories in Livermore, CA has attempted to determine these temperatures using a thermocouple in a laminar-entrained flow reactor. This effort has been unsuccessful, since the high concentrations of

high-temperature CO_2 present in the reactor consume thermocouples used to measure the gas temperatures. Therefore, a new solution for determining the reacting gas temperature, and in turn calculating the kinetic gasification rates, must be utilized. As an attempt at a solution, this report presents the design, construction, and preliminary implementation of a laser Rayleigh scattering (LRS) optical temperature diagnostic, which takes the place of a thermocouple temperature measurement for a flow reactor in the Coal Combustion Lab at the CRF. LRS has been successfully demonstrated as a useful diagnostic for various combustion processes[8,9,10,11]. This optical measurement, in addition to providing temperature information, also preserves the reactor flow characteristics, which is not the case with the thermocouple measurement since it requires the physical placement of the thermocouple inside the reactor.

Theory

Rayleigh scattering is defined as the elastic scattering of electromagnetic radiation from particles much smaller than the wavelength of the incident radiation. Rayleigh scattering is also known as a parametric process, which means that the quantum state of the scattering particle is not changed by the incident radiation, such as it is in inelastic optical mechanisms like Brillouin or Raman scattering. Scattering phenomena are often characterized by what is known as a scattering cross section, which is an effective area that quantifies the probability of a scattering event. For Rayleigh scattering in a gas at STP, the cross section σ_R is given[10] by

$$\sigma_R = \frac{4\pi^2(n-1)^2}{{N_0}^2\lambda^4}\frac{3}{3-4\alpha}\sin^2\theta\,, \tag{1}$$

where n is the index of refraction of the gas, N_0 is the Loschmidt number (2.687 x 10^{19} cm^{-3}), λ is the wavelength of the incident light, α is the depolarization ratio, and θ is the scattering angle. For visible light, Rayleigh scattering typically occurs from atoms or molecules. The most well-known example of this type of scattering takes place in the Earth's atmosphere, which appears blue due to the strong wavelength dependence as seen in Eq. 1. For experimental purposes, the scattering angle θ is often chosen to be 90° in order to maximize the scattered light intensity, and the depolarization ratio α is approximated to zero, simplifying Eq. 1 to

$$\sigma_R = \frac{4\pi^2(n-1)^2}{{N_0}^2\lambda^4}. \tag{2}$$

For a gas mixture, the effective Rayleigh cross section is given by the individual cross sections of the j component gases weighted by the respective mole fraction X_i such that

$$\sigma_R = \sum_{i=1}^{j} X_i\sigma_{R_i}\,. \tag{3}$$

The scattered light intensity I_R is then written as

$$I_R = C_0 I_0 \Omega l N \sum_{i=1}^{j} X_i\sigma_{R_i}\,, \tag{4}$$

where C_0 is an optical calibration constant, I_0 is the incident light intensity, Ω is the solid angle of the collection optics, l is the length of the imaged laser beam segment, and N is the gas number density given by the ideal gas law

$$N = \frac{PA_0}{RT}, \tag{5}$$

where P is the gas pressure, A_0 is Avogadro's number, R is the ideal gas constant, and T is the gas temperature. Since the constants C_0, I_0, Ω, and l are intrinsic characteristics of the optical system used to implement the LRS system, Eq. 4 can be reduced to

$$I_R = CN \sum_{i=1}^{j} X_i \sigma_{R_i}, \tag{6}$$

where C is an optical calibration constant taking into account the incident radiation along with all geometric parameters and optical efficiencies. It can be seen from Eqs. 5 and 6 that

$$I_R \propto \frac{1}{T}, \tag{7}$$

therefore the temperature of a gas or gas mixture with a known cross section can be determined by measuring the Rayleigh scattered light intensity. This principle allows for the application of LRS to combustion diagnostics such as described in this report.

Experiment

A diagram of the experimental setup for LRS measurements of flow reactor gas temperatures is shown in Fig. 1.

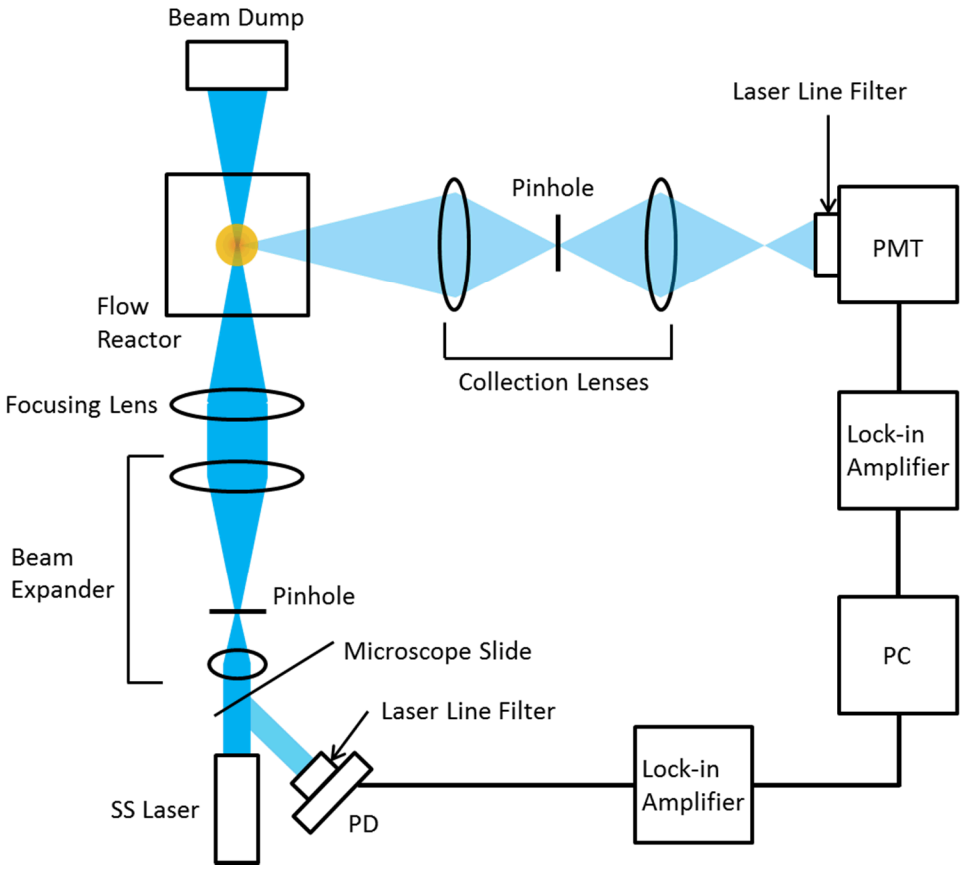

Fig. 1: Diagram of the experimental apparatus designed to measure flow reactor gas temperatures by LRS. The beam from a 165 mW solid state (SS) laser emitting at 490 nm and modulated at 5 kHz by a function generator is passed through a beam expander and focused onto the centerline of a quartz-walled flow reactor. The laser beam is monitored by a line filtered (490 nm peak with a 10 nm full width at half maximum) photodiode (PD) in order to ensure that the optical power incident on the gas is held reasonably constant. A beam dump is placed opposite the laser to collect and dissipate any laser light that is not scattered by the gas in the reactor or by the reactor walls. Collection optics aligned at an angle of 90° collect scattered light for detection by a photomultiplier tube (PMT) which is filtered by the same laser line filter as in front of the PD. Pinholes are used at the input and collection ends in order to clean up the incident beam and to prevent any scattered light not coming from Rayleigh scattering off of the gas to be seen by the PMT. A lock-in amplifier referenced to the function generator going to the laser is used to reduce the noise of the PMT output. Signal data is collected with a computer (PC) for subsequent analysis.

For this LRS diagnostic, the input optical power is supplied by a 165 mW solid state (SS) laser emitting at 490 nm. This laser was chosen instead of a Nd:YAG (532 nm) or HeNe (633 nm) laser since the λ^{-4} dependence on the Rayleigh scattering cross section as seen in Eqs. 1 and 2 states that a shorter scattering wavelength will greatly increase the scattered light intensity shown in Eqs. 4 and 6. The beam from the SS laser is modulated by a function generator which outputs a TTL square wave at 5 kHz. This beam is first partially reflected by a microscope slide in order to monitor the laser output power using a photodiode (PD) which is filtered by a laser line filter with a 490 nm peak and 10 nm full width at half maximum (FWHM) in order to only measure the reflected laser light and not any background light at different wavelengths. The PD output is sent to a lock-in amplifier, which is referenced by the function generator modulating the laser. The beam then passes through a ~4x beam expander created by 50 mm and 200 mm focal length lenses. At the focal point of the beam expander, a 200 µm pinhole is inserted in order to prevent any unwanted beam artifacts from further propagating through the optical train. A

focusing lens with a focal length of 150 mm is placed after the beam expander in order to focus the beam onto a small point at the centerline of the flow reactor. The practice of expanding and then focusing the beam is done in order to minimize the beam waist, or the width of the beam at its narrowest point, at the reactor centerline, which allows for a more precise Rayleigh scattering image to be projected onto the collection optics. The walls of the reactor are made of quartz, a transparent material that has an extremely low thermal expansion coefficient, in order to provide optical access into the reactor and minimize any shifting of the reactor during high temperature reactions. The laser light that is not either scattered by the gases in the reactor or by the reactor walls is collected and dissipated by a beam dump opposite the laser.

In order to collect the maximum amount of Rayleigh scattered light, the collection optics for the LRS system are placed at a scattering angle of 90^{o} in accordance with Eq. 1. A collection lens is placed as close to the center of the reactor as possible in order to maximize the solid angle Ω in Eq. 4. The lens has a relatively short focal length (75 mm) in order to minimize the f-number to a value of 1.5, which also maximizes the collected light intensity. The collected scattered light is then focused through a 150 μm pinhole, which eliminates some of the extraneous light from scattering off of areas other than the focal point of the beam at the center of the reactor. The resulting light is then imaged onto the cathode of a photomultiplier tube (PMT). A PMT was selected due to its high sensitivity and high signal-to-noise ratio compared to other low-light detectors such as amplified or avalanched photodiodes. Since Rayleigh scattering is an elastic process, another 490 nm (10 nm FWHM) line filter is placed in front of the PMT in order to maximize the ratio of Rayleigh scattered light to background light detected by the PMT. The output of the PMT is sent to a lock-in amplifier, which is referenced by the function generator that modulates the laser. Lock-in amplifiers are used for the outputs of the PD and the PMT in order to improve the signal-to-noise ratio and eliminate an offset due to background light. Lock-in amplifiers are phase-sensitive detectors which effectively act as band pass filters that output a voltage proportional to the signal level it detects that also matches an input reference frequency. Therefore, the only signal levels output from the lock-in amplifiers are due to light incident on the PD and the PMT from either scattered laser light (from the background) or Rayleigh scattered light from the gases in the reactor. The voltages output by the lock-in amplifiers are sent to a data acquisition board which communicates with a computer (PC). The computer uses custom data collection software written in LabVIEW to output raw data files to be further analyzed.

The experimental procedure for the proposed LRS system involves several steps in addition to measuring scattered light signals. In order to correlate the measured signal levels to temperature measurements, the optical calibration constant C from Eq. 6 must first be determined. This was done by measuring reference scattering signals from flowing pure N_2 and CO_2 in the reactor. Next, a Hencken burner at the bottom of the flow reactor was lit in a 12% O_2 reaction environment. The scattered light from this flame was measured, along with scattering from N_2 and CO_2 in order to calculate a scattering background signal, for a series of selected heights inside the reactor, which has a total height of 18 inches. The interpretation of these measurements is further explored in the “Analysis and Results” section.

Analysis and Results

In order to analyze the raw signals collected from N_2, CO_2, and the 12% O_2 flame, a data analysis algorithm was developed in order to correlate the measurements to temperatures. For a given signal R measured by the PMT in the proposed LRS system, it can be said that

$$R = I_R + S_B \,, \tag{8}$$

where I_R is the measured signal due to Rayleigh scattering from a gas and S_B is the signal due to background scattering of light off of the quartz reactor walls, optical components, and other reflective surfaces in the optical train. From Eqs. 6 and 7, it is true that

$$I_R = C\frac{\sigma_R}{T}\,, \tag{9}$$

since C is an undetermined calibration constant. Therefore, using the measured reference signals R_{N_2} and R_{CO_2} from N_2 and CO_2 and the fact that

$$\sigma_{CO_2} = 2.4\sigma_{N_2}, \tag{10}$$

C can be calculated from

$$C = \frac{R_{CO_2} - R_{N_2}}{1.4/T_{cal}}\,, \tag{11}$$

where T_{cal} is the temperature at which the calibration is performed, which was room temperature for this experiment. Once the calculation of C is performed, the flame signal R_{flame} and the reference signals collected at each selected reactor height are used to determine background scattering levels S_B by

$$S_B = \frac{2.4R_{N_2} - R_{CO_2}}{1.4}\,, \tag{12}$$

and finally the flame temperature T by

$$T = \frac{C\sigma_{flame}}{R_{flame} - S_B}\,, \tag{13}$$

where σ_{flame} is the Rayleigh scattering cross section of the combustion products (relative to the scattering cross-section for nitrogen).

In order to illustrate the typical data collection and analysis used in this diagnostic, an example measured signal time series collected from the LRS system is shown in Fig. 2.

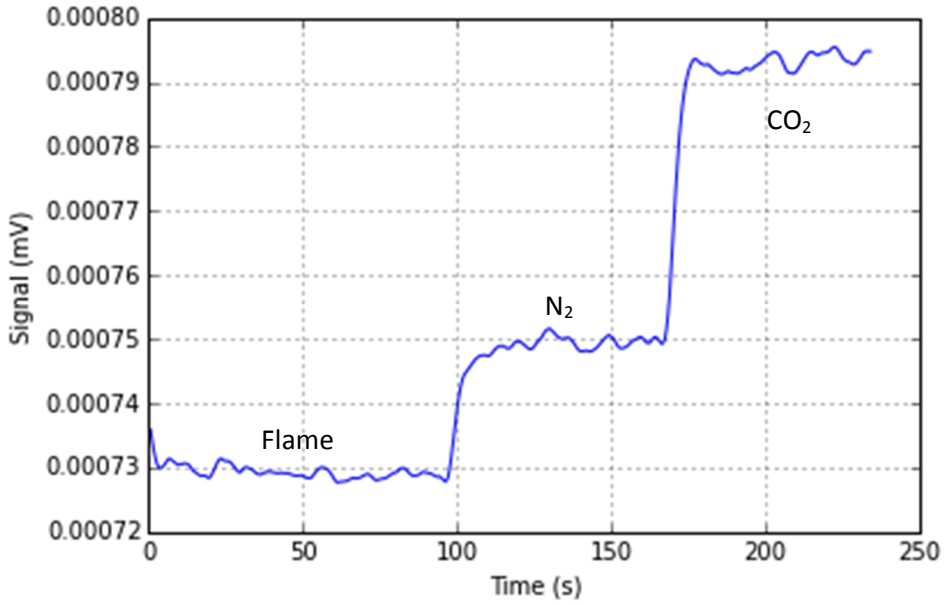

Fig. 2: Example measured signal time series using the LRS system in Fig. 1 for a given reactor height. The lowest signal level represents the time at which the flame in the flow reactor is lit, the middle signal around 0.75 µV occurs when N_2 is flowing in the reactor, and the highest signal occurs when CO_2 is flowing.

Fig. 2 represents an example data point from an attempt to create a temperature profile as a function of height above the Hencken burner for the centerline in the flow reactor. First, the flame is lit, then the flame is extinguished and N_2 is flowed into the reactor, then the N_2 is turned off and CO_2 is flowed. The differences in the signal between the N_2 and CO_2 signals is assumed to be solely due to the difference in the scattering cross sections, while the difference between the references and the flame signal is due to the scattering cross section of the combustion products as well as the increased temperature of the flame. From this time series, the signal levels for each case can be determined by averaging the data over the time for each reactor environment state. Further, the uncertainty in the determination of the signal levels can be reduced by fitting the data to linear functions using a least squares fit, then correcting the differences between the signals for any slope that may have been introduced from a drift in the background scattering signal due to the heating or cooling of the flow reactor. Such analysis can be seen more clearly in Fig. 3.

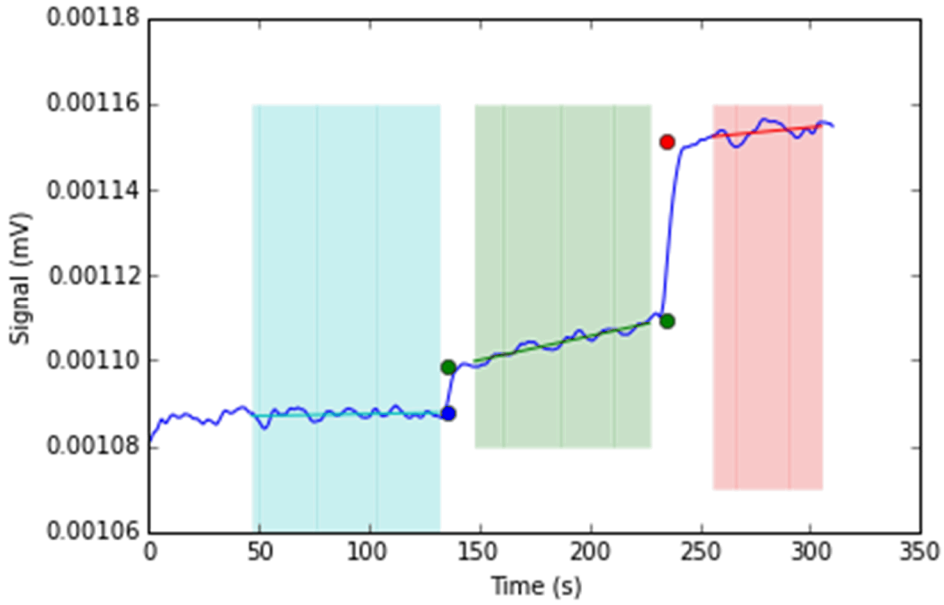

Fig. 3: Example measured signal time series displaying a slope due to a shift in the background scattering signal, possibly caused by cooling of the reactor after the flame was extinguished. This was corrected for by performing a least squares fit to the data for each reactor state, shown in the figure as blue, green, and red lines. While this analysis technique decreased the uncertainty in each measurement, the accuracy was not improved. The least squares analysis software was developed in Python.

From each of these time series collected for selected reactor heights, values for R_{flame}, R_{N_2}, and R_{CO_2} can be determined. Then using Eqs. 12 and 13, along with the previously determined C from Eq. 11, the scattering background S_B and flame temperature T can be determined. However, results that have been obtained from this method have not been successful in determining accurate temperature measurements. Fig. 4 shows a measured reactor temperature profile for the 12% O_2 reaction environment plotted with temperature data obtained using a thermocouple.

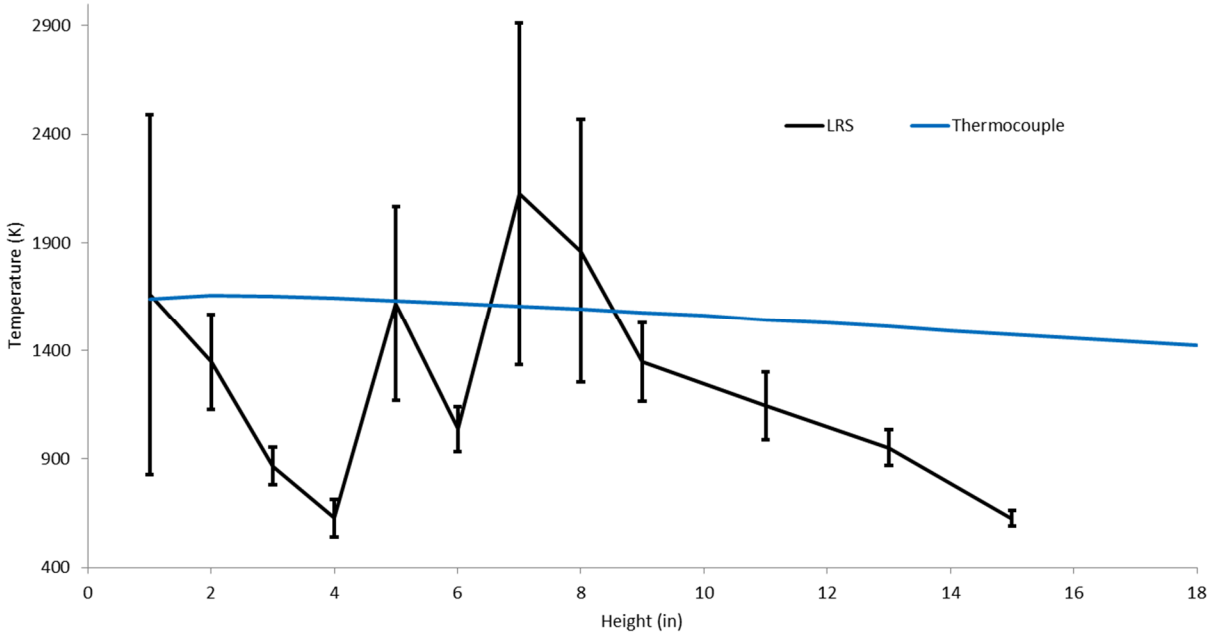

Fig. 4: Measured temperature profile from the LRS system plotted with the reactor temperature profile measured by a thermocouple for a 12% O_2 flame environment. It can be seen that there is a large amount of inaccuracy in the LRS temperature measurements relative to the thermocouple measured temperatures. The uncertainties in these measurements can be reduced by the linear regression technique from Fig. 3, but was not performed here since the LRS measurements would no longer be within uncertainty to the thermocouple data.

The results in Fig. 4 indicate that the LRS diagnostic is currently not capable of obtaining accurate temperature measurements, and it is unclear why this is the case.

Discussion

At the present time, this diagnostic is still being developed. It can be clearly seen in Fig. 4 that the LRS system is not currently capable of determining accurate reactor temperatures for the study of oxy-combustion of coal char. From the data in Figs. 2 and 3 it can be seen that the measured signal levels are small, on the order of 1 μV. While this is expected from a photomultiplier tube used with sufficient extraneous light rejection, it was realized from calculations using Eqs. 9 and 12 and the measured signal data that less than 1% of the signals could be attributed to Rayleigh scattering. This causes problems for the LRS diagnostic since only a small relative change in the background scattering level can greatly change the calculated Rayleigh signal level, which is the only portion of the measured signal that is a predictable function of temperature. Future work will likely include finding a way to reduce this background scattering to an acceptable level in order to increase the accuracy of the Rayleigh temperature measurements for the 12% O_2 flame, and then an attempt to apply the diagnostic to high-temperature CO_2 gasification of coal char would be taken once a sufficient level of accuracy is achieved. Also, it has been hypothesized that the background scattering level may be a function of the relative cross sections of each of the calibration gases and the combustion products, which may be skewing the resulting temperatures. This hypothesis will also be explored in the future.

Conclusion

In this report, the design and testing over 8 weeks of a laser Rayleigh scattering temperature diagnostic with the goal of studying oxy-combustion of coal char was presented. The diagnostic system was constructed to measure Rayleigh scattered light from gases inside an optically-accessible laminar entrained flow reactor. Signals were measured using the LRS system and data collection and analysis algorithms were developed in order to correlate the measured signals to temperatures. Preliminary results have shown that the LRS system does not provide accurate temperature measurements, and it is unclear at the present time why this is.

References

[1]Fourier, J. B. J., 1824. Remarques Générales Sur Les Températures Du Globe Terrestre Et Des Espaces Planétaires. *Annales de Chimie et de Physique* 27:136–167.

[2]Intergovernmental Panel on Climate Change (IPCC), 2014. IPCC Fifth Assessment Report.

[3]U.S. Energy Information Administration (U.S. EIA), 2015. Annual Energy Outlook 2015.

[4]Buhre, B.J.P., Elliott, L.K., Sheng, C.D., Gupta, R.P., & Wall, T.F., 2005. Oxy-fuel combustion technology for coal-fired power generation. *Prog. Energy Combust. Sci.* 31:283–307.

[5]Toftegaard, M.B., Brix, J., Jensen, P.A., Glarborg, P., & Jensen, A.D., 2010. Oxy-fuel combustion of solid fuels. *Prog. Energy Combust. Sci.* 36:581–625.

[6]Power Plant CCS, 2010. Oxy Fuel Combustion Method. http://www.powerplantccs.com/ccs/cap/con/of/of.html. Accessed July 27, 2015.

[7]Hecht, E.S., Shaddix, C.R., Molina, A., & Haynes, B.S., 2011. Effect of CO_2 gasification reaction on oxy-combustion of pulverized coal char. *Proc. Combust. Inst.* 33:1699-1706.

[8]Pitz, R.W., Cattolica, R., Robben, F., & Talbot, L., 1976. Temperature and Density in a Hydrogen-Air Flame From Rayleigh Scattering. *Comb. Flame* 27:313-320.

[9]Dibble, R.W., & Hollenbach, R.E., 1981. Laser Rayleigh thermometry in turbulent flames. *Symposium (International) on Combustion* 18:1489-1499.

[10]Zhao, F. & Hiroyasu, H., 1993. The applications of laser Rayleigh scattering to combustion diagnostics. *Prog. Energy Combust. Sci.* 19:447-485.

[11]Miles, R.B., Lempert, W.R., & Forkey, J.N., 2001. Laser Rayleigh scattering. *Meas. Sci. Technol.* 12:R33.